SEA ICE CLASSIFICATION ON DIFFERENT SPATIAL SCALES FOR OPERATIONAL AND SCIENTIFIC USE

Wolfgang Dierking [(1)]

[(1)] *The Alfred Wegener Institute, Helmholtz Centre for Polar and Marine Research, Bussestr. 24, 27570 Bremerhaven, Germany, Email: Wolfgang.Dierking@awi.de*

ABSTRACT

With the possibility of acquiring satellite radar images at different spatial resolutions and swath widths (i. e. at different scales) there is a need for selecting the optimal image product for the analysis of sea ice conditions. Both resolution and areal coverage influence the discrimination (and definition) of different sea ice zones and structures. A wide coverage is usually linked with a relatively coarse spatial resolution, whereas high-resolution products are restricted to narrow swath widths. Examples are presented which demonstrate pros and cons when balancing both parameters for the analysis of sea ice conditions. It is shown that X- and C-band images reveal similar signature variations (except over thin ice) and are hence well suited for combining images taken at different scales. Cases were observed for which strongly averaged intensity images are beneficial for discriminating different ice zones. For making full use of texture analysis, higher resolution products are preferable.

1. INTRODUCTION

The term "scale" is closely linked to the spatial resolution and areal coverage of an image acquired over the Earth's surface. It is a characteristic of the "filter" through which a scene is perceived, besides other sensor properties and the imaging geometry used for data acquisition. The choice of the appropriate scale (resolution and coverage) depends on the desired output information, the method for retrieving the information, and the spatial structure of the scene [1]. The possibility to classify different units on the Earth's surface, and the quality/accuracy of the classification is determined by the information content of the image. Here we concentrate specifically on the analysis and mapping of sea ice conditions using synthetic aperture radar (SAR) images acquired at different spatial resolutions and swath widths. For a general introduction to sea ice monitoring by SAR, the reader is referred to [2].

The information in radar images is carried as spatial variations of intensity and phase. In the latter case it is the phase difference between the HH- and the VV-polarized channel, which may be useful for sea ice classification ('HH' means that transmitted and received signal are horizontally polarized, 'V' stands for 'vertical'). In this paper, however, the phase difference is not considered.

Regarding the information content of an image, the central question is whether there is a link or correlation between the directly measured quantity (e. g. radar intensity) and the geophysical parameter that shall be retrieved (e. g. ice type). Provided that this is the case, the ratio between the spatial extent of sea ice zones or the sizes of sea ice structures, on the one side, and the image resolution and coverage, on the other side, influences the result of the classification. This is the topic of this paper. For completeness it is noted that the information content of a SAR image depends also on the radar frequency, polarization, incidence and azimuth angles, signal-to-noise ratio, and image pre-processing (e. g. speckle filtering).

2. VISUAL ANALYSIS OF SAR IMAGES

For the separation of ice types, it is often useful if certain ice structures can be identified unambiguously in the SAR image (e. g. rafting indicates that the ice is thin). In Fig. 1, a zoom-in of an ASAR wide-swath (WS) scene with a spatial resolution of 150 m is compared to an airborne SAR image with a 2 m-resolution. The data are from a sea-ice-covered area in Fram Strait northeast of Svalbard, acquired in March 2007 during the ICESAR campaign [3]. In the airborne image, ridges on the thicker ice floes (light green) are visible as well as rafting structures in thin ice (dark green). Edges of floes, cracks and leads appear as sharp boundaries. At the resolution of 150 m, ridges and rafting patterns or leads and cracks cannot be recognized, and the edges of floes are blurred. While it is possible in the ASAR wide-swath scene to distinguish thicker ice floes from the thinner ice surrounding them, the degree of deformation (which is related to the number and spacing of ridges and rafting zones) cannot be assessed. Without any further information it is even difficult to decide whether the dark background in the ASAR image is open water or thin ice.

In the example provided in Fig. 2, an ASAR wide-swath image is analysed in combination with a TerraSAR-X (TSX) stripmap image. The data were acquired over the Beaufort Sea. The ASAR scene, processed with a pixel size of 150 m and a coverage of 400 km × 400 km, is part of a sequence of images that were used to study the effect of melt-onset on the radar signature [1]. The

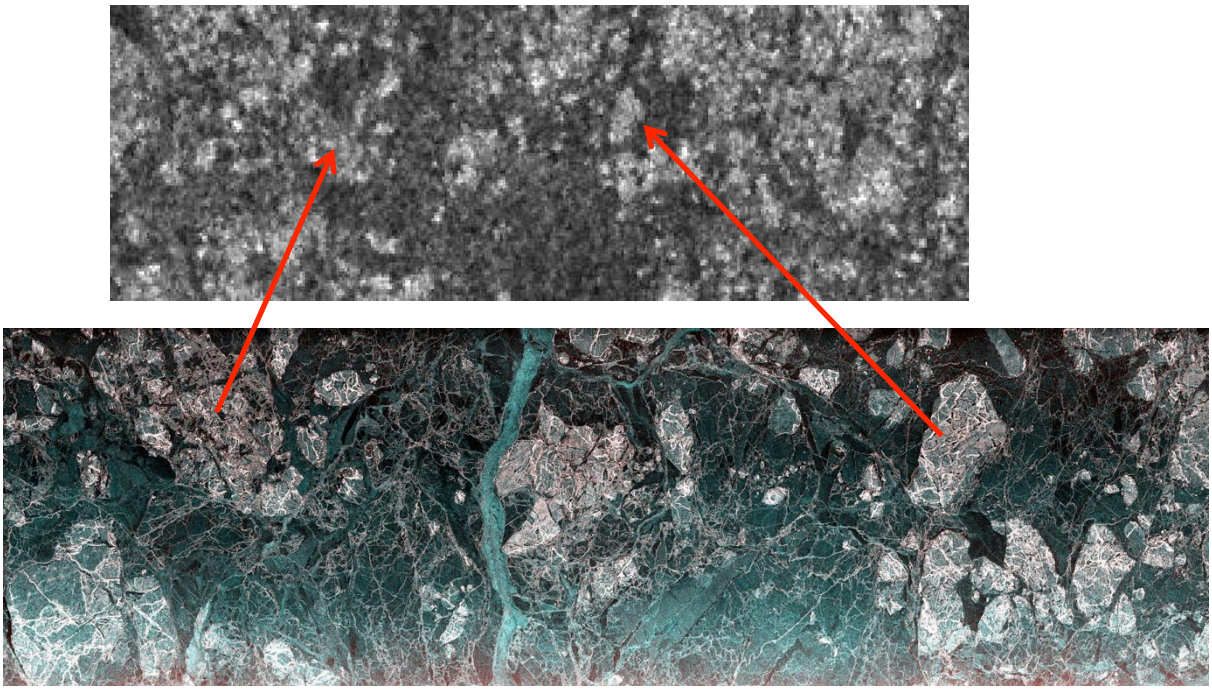

Figure 1. The effect of spatial resolution. Top: ASAR WS, 19/03/2007, 11:22 UTC, HH-polarization. Bottom: airborne SAR (German Aeropspace Center), same day, 12:26 UTC, swath width: 3 km. The RGB colour-layers indicate polarization: R-VH, G-HH, B-VV. For ease of allocation, two of the ice floes appearing in the airborne and WS image are connected by arrows.

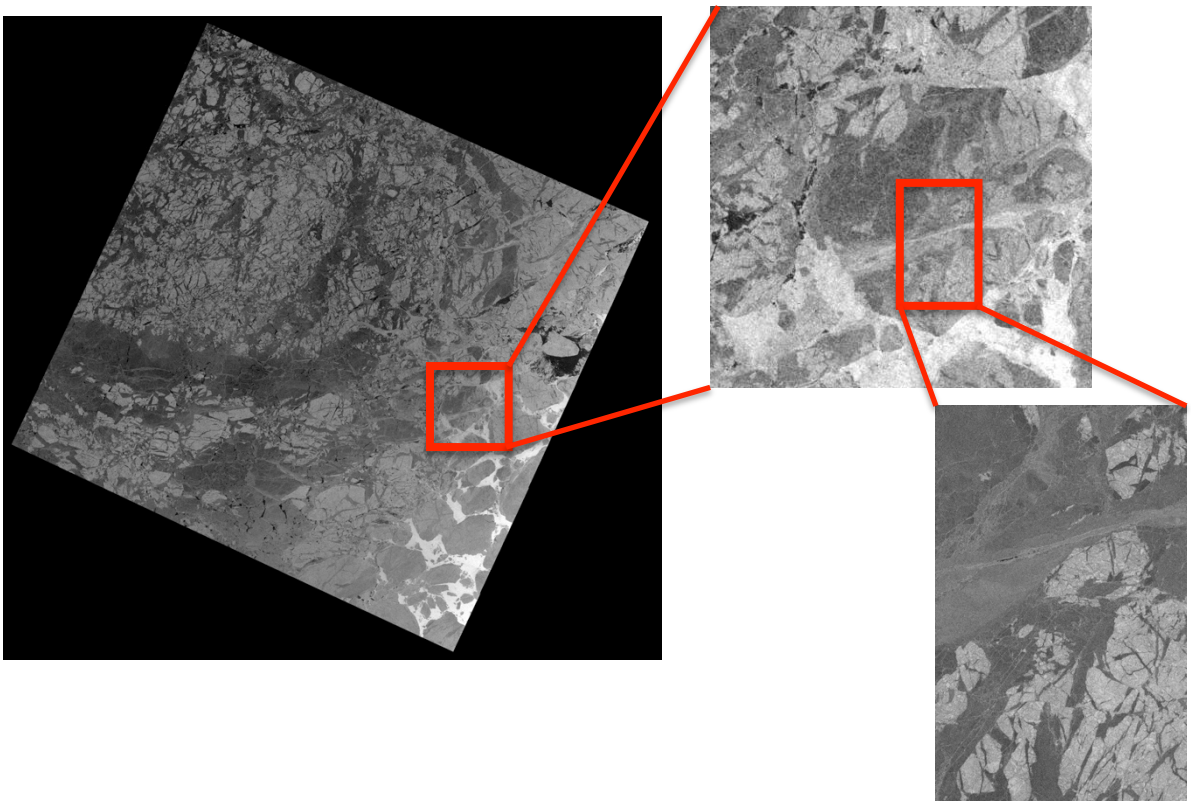

Figure 2. The effect of swath width. Left: ASAR WS 02/06/2008, 20:27 UTC, HH-polarization, swath width 400 km. Upper right: zoom-in of ASAR scene, lower right: TSX SM 02/06/2008, 16:06 UTC, HH-polarization, width 15 km.

pixel size of the TSX-image is 20 m after geocoding and calibration, and the swath width is 15 km. Again, small and narrow ice structures (ridges, rafting zones, refrozen leads) can only be identified in the high-resolution TSX-image. However, over scales of tens of kilometres, different sea ice zones can be recognized in the wide-swath ASAR image, e. g. the ice margin consisting of larger ice floes and open water patches to the lower right of the scene, larger elongated areas of thinner ice (dark grey) in the lower third, and an area of ice broken into several pieces in the left top half. This is an example in which C- and X-band imagery acquired at different spatial resolution can be used in combination for a more detailed analysis of the ice conditions than would be possible if only one of these images is available. This is discussed in more detail in section 4.

3. WHY LOOK AT DIFFERENT SCALES?

The availability of imagery with different resolutions and coverage is of advantage not only for sea ice mapping and ice type classification. In this section, we briefly discuss the relevance of the topic for the retrieval of *sea ice drift* patterns and the derivation of *scaling laws*.

For calculating *sea ice drift*, so-called "resolution pyramids" are constructed. The original high-resolution scene is low-pass filtered to generate a sequence of images with decreasing spatial resolution. The initial drift vectors are then computed using the image with the coarsest resolution, representing a large-scale, not very detailed view of the drift pattern. The results obtained at coarser resolution are used to start the calculations of drift vectors on the next finer resolution level down to the original high-resolution at which the most detailed drift pattern is obtained [4]. Usually, only image sequences acquired at a fixed imaging mode of a selected satellite SAR are employed for drift calculations. This means that the temporal gaps between successive images are relatively large. One solution to reduce the time gaps is to combine data from different sensors and imaging modes, e. g. interferometric or extra wide-swath mode from Sentinel-1 and ScanSAR mode from TSX. One necessary condition for combing data from different SAR-systems is that ice cover zones and structures appear similar in the used image types since it is necessary to follow their changes of position between successive images. Differences of the spatial resolution between the two images used as input to the drift calculation procedure are balanced in the resolution pyramid. Whether the combination of different image types is useful depends also on the total areal coverage of each type. Results of such a combined approach have not been published yet.

Another interesting application of combining images acquired at different spatial resolutions is the derivation or validation of *scaling laws*. Certain sea ice parameters can be expressed as a function of scale (e. g. size, length, width, distance) [5]. Scaling laws were found, e. g., for the total sea ice strain rate (the combination of shear and divergence) [5, chapt. 3.2], size of ice floes [5, pp. 62-63], width of leads [5, p. 64], and fraction of open water [5, p. 64]. In a compact sea ice cover, e. g., the number of ice floes N of a given size s follows a power law $N \sim s^{-\alpha}$, with $\alpha \approx 3$ [5, p.7]. If the number of ice floes in a given size interval is known, it can be calculated also for a different range of sizes. This means that a coarse-resolution image is sufficient for counting the number of larger floes (and to find or validate the coefficient α) and from this to calculate the number of smaller floes even if they are too small to be separated as distinct objects in the image. (A problem, however, is to decide whether a "large floe" seen at coarse resolution is in fact a single floe or composed of different smaller floes). In SAR images, ice ridges appear as narrow linear structures on the ice. If the spatial resolution is too coarse, they "vanish". Hence, the results of retrieving areal fraction of deformed ice and distance between zones of deformation depend on the image resolution [6]. It was found that scaling factors can be applied to calculate the areal fraction and distances of deformation zones at a selected spatial resolution when using L-band SAR images. The investigations presented in [6] were, however, restricted to a narrow range of pixel sizes (5-25 m).

4. COMBINING C- AND X-BAND

To study the effect of spatial resolution on the classification accuracy, a high-resolution image can be used to generate a resolution pyramid (see section 3) and apply the selected classification algorithm to each resolution level [7]. In this article, we focus on another scenario, in which images acquired by different sensors are combined, making use of their respective advantages for sea ice mapping, dependent on frequency, polarization, incidence angle, spatial resolution and aeral coverage. This scenario is relevant for operational sea ice monitoring.

In former studies it was recognized that sea ice often appears similar in SAR images acquired at C- and X-band. Since the X-band images are usually available at a higher spatial resolution and C-band images at a wider coverage when using comparable imaging modes (e. g. wide-swath and ScanSAR), we expect that their combination is most beneficial if the equivalence of the information content is a requirement. To investigate this, we compared a Radarsat-2 (RS2) quad-polarization mode with a TSX dual-polarization stripmap (SM) mode (Fig. 3). The specifications for the RS2 scenes in Fig. 3 are: VV-polarization, acquired on 03/06/2008 15:43 UTC, pixel size 20 m, incidence angle 40.1-40.7 deg, equivalent number of looks ENL≈20. The corresponding data for the TSX image sections are: VV-

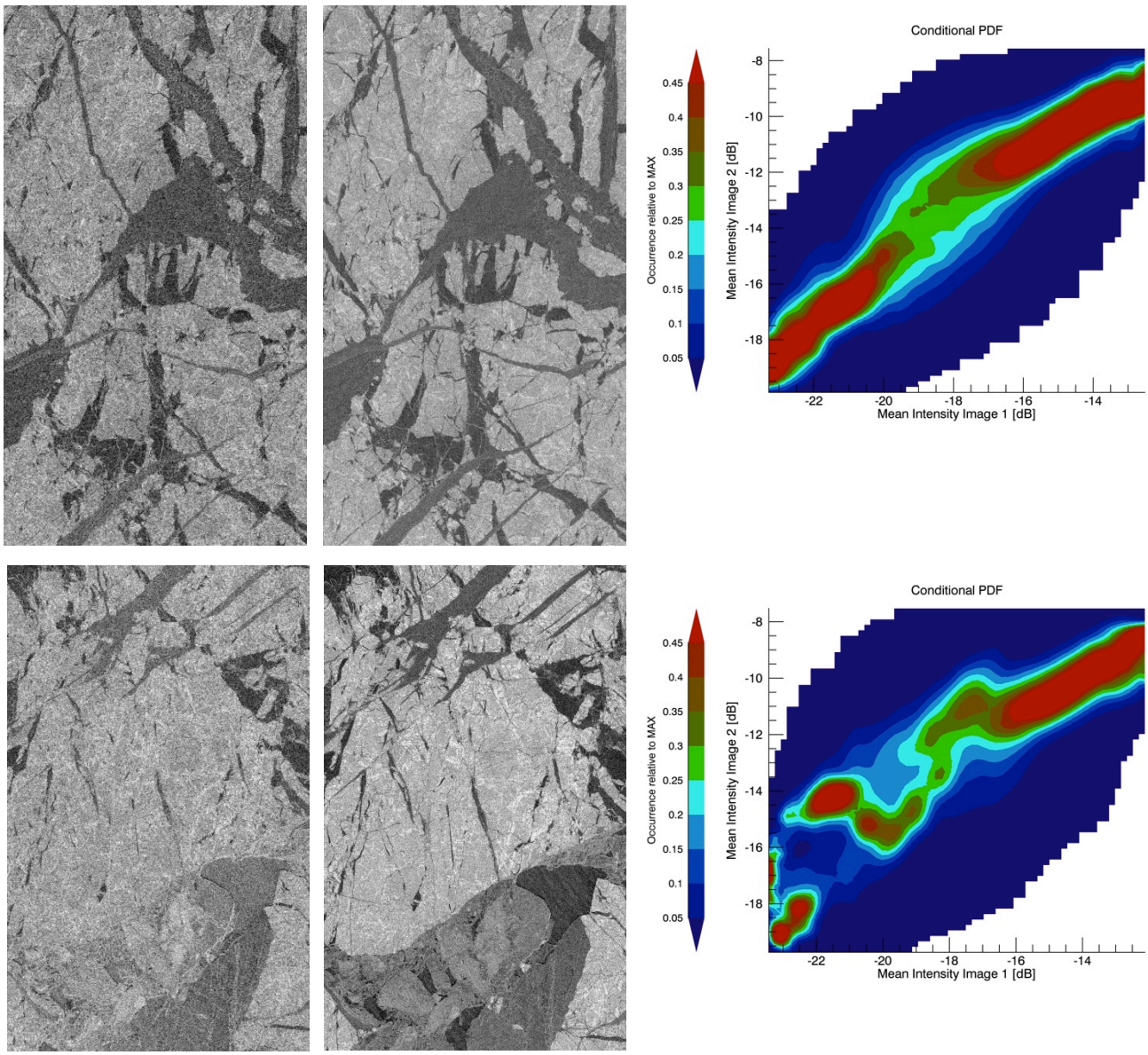

Figure 3. Equivalence of C- and L-band. Left: Two sections from an RS2 image acquired in the Beaufort Sea during the MELTEX 2008 campaign, width of scene 9 km; middle: the two corresponding sections from TSX; right: discrete conditional 2-D PDF, where image 1 (x-axis) is the TSX- and image 2 (y-axis) the RS2-scene.

polarization, 03/06/2008 15:49 UTC, pixel size 20 m, incidence angle 41.1-42.1 deg, ENL>50. With ENL>20, the contribution of speckle is low. It is considerably more supressed in the TSX- than in the ASAR-image.

How can the equivalence between X- and C-band data be assessed? We chose an approach described in [8] and [9], which uses the discrete conditional two-dimensional probability density function (2-D PDF), which shows whether the information content of image 1 can be reconstructed from image 2 [9].

The upper sections of the RS2 and TSX images depicted in Fig. 3 resemble one another, which is also reflected in the conditional PDF to the right. A perfect correspondence between the information content of the two images results in straight contour lines from the lower left to the upper right of the plotted PDF. This is almost fulfilled here. (Note that the absolute level and range of backscattered intensities differ between C- and X-band. The important point is that the conditional PDF can be used to reconstruct the second from the first image.) For the lower image sections, however, the situation is different. The lower third of these sections covers an area of thin ice and open water. The appearance of this area differs between C-band (RS2, to the bottom left of Fig. 3) and X-band (TSX, bottom middle). The corresponding conditional 2-D PDF shows a more complex shape for lower values of the backscattered intensities. The results presented here demonstrate that C- and X-band SAR images of sea ice do not reveal a one-to-one correspondence, but are

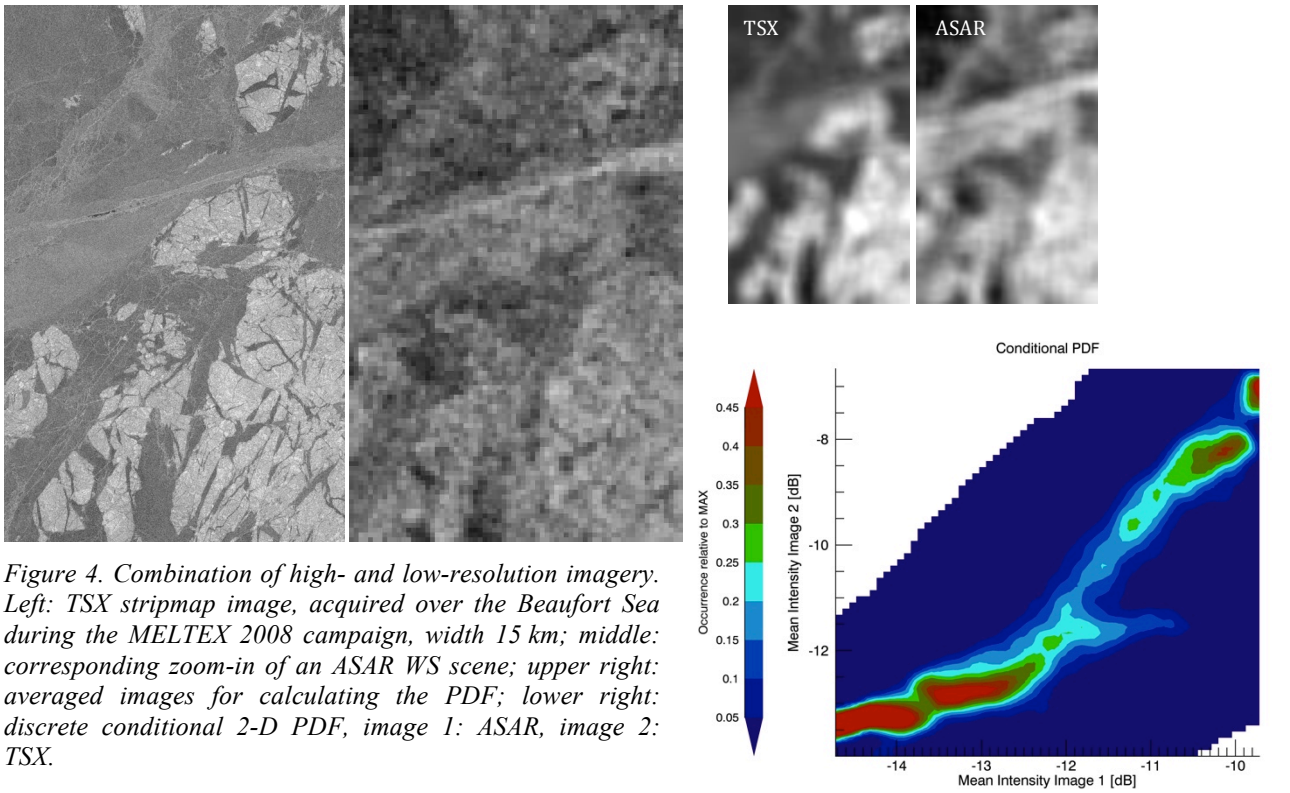

Figure 4. Combination of high- and low-resolution imagery. Left: TSX stripmap image, acquired over the Beaufort Sea during the MELTEX 2008 campaign, width 15 km; middle: corresponding zoom-in of an ASAR WS scene; upper right: averaged images for calculating the PDF; lower right: discrete conditional 2-D PDF, image 1: ASAR, image 2: TSX.

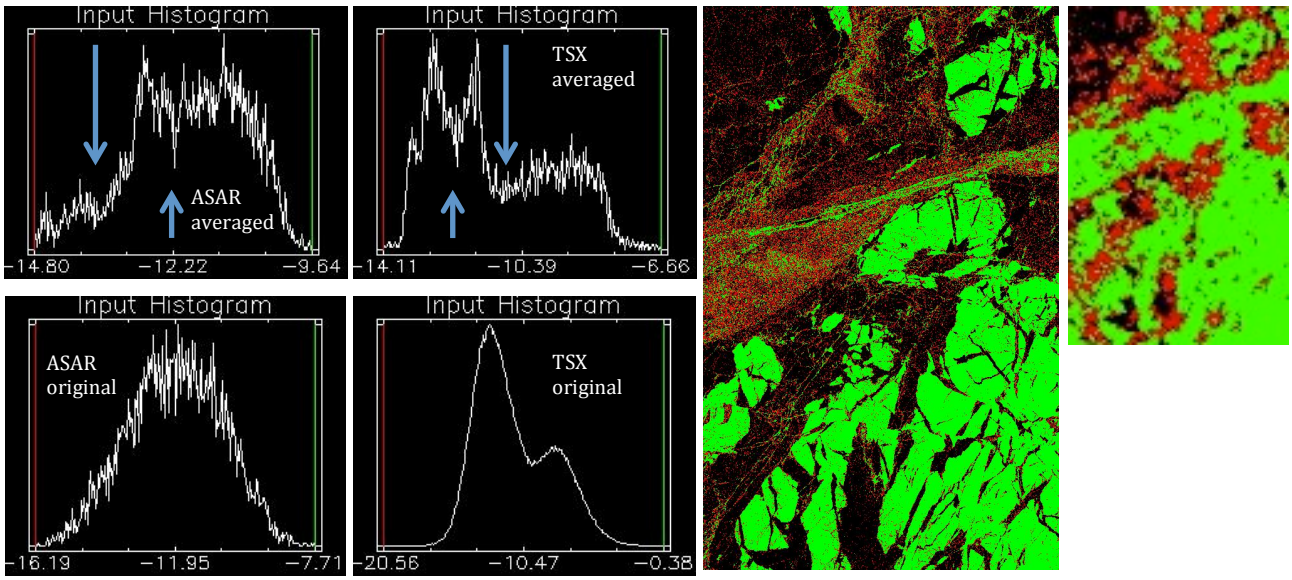

Figure 5. Separation of sea ice classes based on averaged images. Left: Histograms of averaged (upper row) and original (lower row) histograms. Arrows indicate positions of thresholds determined by local minima. Right: classified images (discussed in the text).

sufficiently similar over thicker consolidated ice in many cases, whereas larger differences may appear over new ice. For special surface conditions such as the occurrence of frozen snow crusts, snow ice, or superimposed ice, we suspect that C- and X-band radar signatures will reveal non-negligible differences also over thicker ice.

5. COMBINING COARSE- AND HIGH-RESOLUTION IMAGERY: INTENSITY

In the next step, we combined a TSX dual-polarization SM and an ASAR WS image. (Fig. 4). The TSX image was acquired on June 2, 2008 at 16:06 UTC. We used the HH-polarized data, processed with a pixel size of

20 m, ENL≈20 and an incidence angle range from 34.6 to 35.1 deg. The ASAR scene is from 20:28 UTC, HH-polarization, pixel size 150 m, and ENL>100. The incidence angle range of the zoom-in corresponding to the area covered by the TSX image is 22-22.4 deg. In the ASAR zoom-in it is difficult to separate ice classes (Fig. 4). The TSX image is very useful to interpret the signature variations in the ASAR scene and to link radar intensities and texture with ice types (including the possibility to extend the interpretation over areas in the ASAR frame that are not covered by TSX-data). Again the question arises whether the information contents at C-band (ASAR) and X-band (TSX) are equivalent? To answer this question, both images were averaged. We selected a window of 7 pixels in the ASAR scene, and fixed the window size for the TSX image correspondingly to 53 pixels. Whereas the window was moved pixel-by-pixel in the ASAR scene, it was centred on every 7th pixel when sliding through the TSX scene. The results are depicted in Fig. 4 to the upper right. Differences occur in the zone of the lead (running from the left to the right in the upper third of the images) and in the thin ice areas. The latter appear all dark in the TSX-image, whereas they are more patchy with varying grey tones in the ASAR scene. The difference in the radar intensities may be caused by the different radar frequencies and/or the time gap of 4.5 hours between data takes. The associated conditional 2-D PDF reveals that there is a systematic relation between the C- and X-band intensities although C-band intensities for thin ice show larger variations than at X-band. The result indicates that the coarse-scale information content of the two images is equivalent.

Looking at the intensity histograms of the two full-resolution images (Fig. 5 bottom row left), it is not possible to distinguish different sea ice classes in the ASAR scene, and only two classes can be discriminated in case of TSX. Using the averaged images, the situation changes. Now three different classes can be separated in both cases (although it is more difficult for ASAR). In fact, [1] reported that in many situations, the use of successively higher spatial resolution resulted in lower overall classification accuracy because of the within-class variability. Hence, the separation of different sea ice zones (each extending over larger areas covering several pixels) can be easier when using highly averaged data for fixing the thresholds between ice classes. The thresholds are then applied to the original image. This is demonstrated in Fig. 5, in which the results of classifying the TSX and ASAR scene are shown in the right part. Note the differences in the zone of lead ice and in the thin ice area, which correspond to the variations in grey tones discussed above. Whether different ice classes are easier to separate in the histograms of averaged images depends on the window size used for averaging and on the spatial extension of different sea ice zones and structures.

6. COMBINING COARSE- AND HIGH-RESOLUTION IMAGERY: TEXTURE

For classification of sea ice types, not only the mean intensity values can be used, but also the image texture. In the former case, we consider variations of the measured intensity that occur on length scales much larger than the pixel size. Thus we distinguish different extended zones in the image (‘zonal classification’). These zones may be superimposed by structures that are only 1-2 pixels wide or cover only a few pixels (for sea ice, e. g.: ridges, rafting patterns, cracks, narrow leads, brash ice). These structures may reveal homogeneous or inhomogeneous patterns and can be characterized by different textural parameters [10]. It is obvious that the identification of typical sea ice structures depends on the spatial resolution of the SAR image.

In Fig. 6 (top), two SAR image are shown that were acquired over the western Weddell Sea on February 23, 2010. One is an ASAR WS scene (100 m pixel size, HH-polarization, 04:01 UTC), the second one is the ScanSAR mode from TSX (30 m pixel size, HH-polarization, 23:40 UTC). The covered region consists of first-year ice with shear zones, cracks, and open water patches. The latter are visible in both images, whereas the linear structures (shear zones and cracks) can hardly be identified in the ASAR image. The brightest objects in the scene are icebergs, which can be recognized in both scenes, as well as a few ice floes appearing black (to the upper right). The standard deviation was calculated in a sliding window (window sizes ASAR 7 pixels, TSX 23 pixels, sliding distance ASAR 1 pixel, TSX 3 pixels). The contours of the icebergs, the dark floes, and the open water patches appear in both texture patterns (Fig. 6, bottom), whereas linear elements linked to shear zones and cracks are only visible in the result from TSX. Although we have to consider the different frequencies and the time difference of 19.5 hours between image acquisitions, this example demonstrates that spatial resolutions of about 5-30 m (dependent on the number of looks) are required to identify typical structure elements of a sea ice cover and to include them in classification. (We note that there may be situations of mapping for which it is of advantage to minimize the influence of those structures on classification, see above).

7. DISCUSSION

The spatial resolutions of SAR images required for a certain mapping task are listed in different reports. In cryospheric research [11], the ‘goal’ for classification is to separate ice types on length scales of 5 km (corresponding to the zonal classification approach discussed above). This can be achieved with a spatial resolution on the order of 100 m, which is typical for WS imaging modes. Ice displacement vectors should ideally be provided on grids of 1 km width. This means

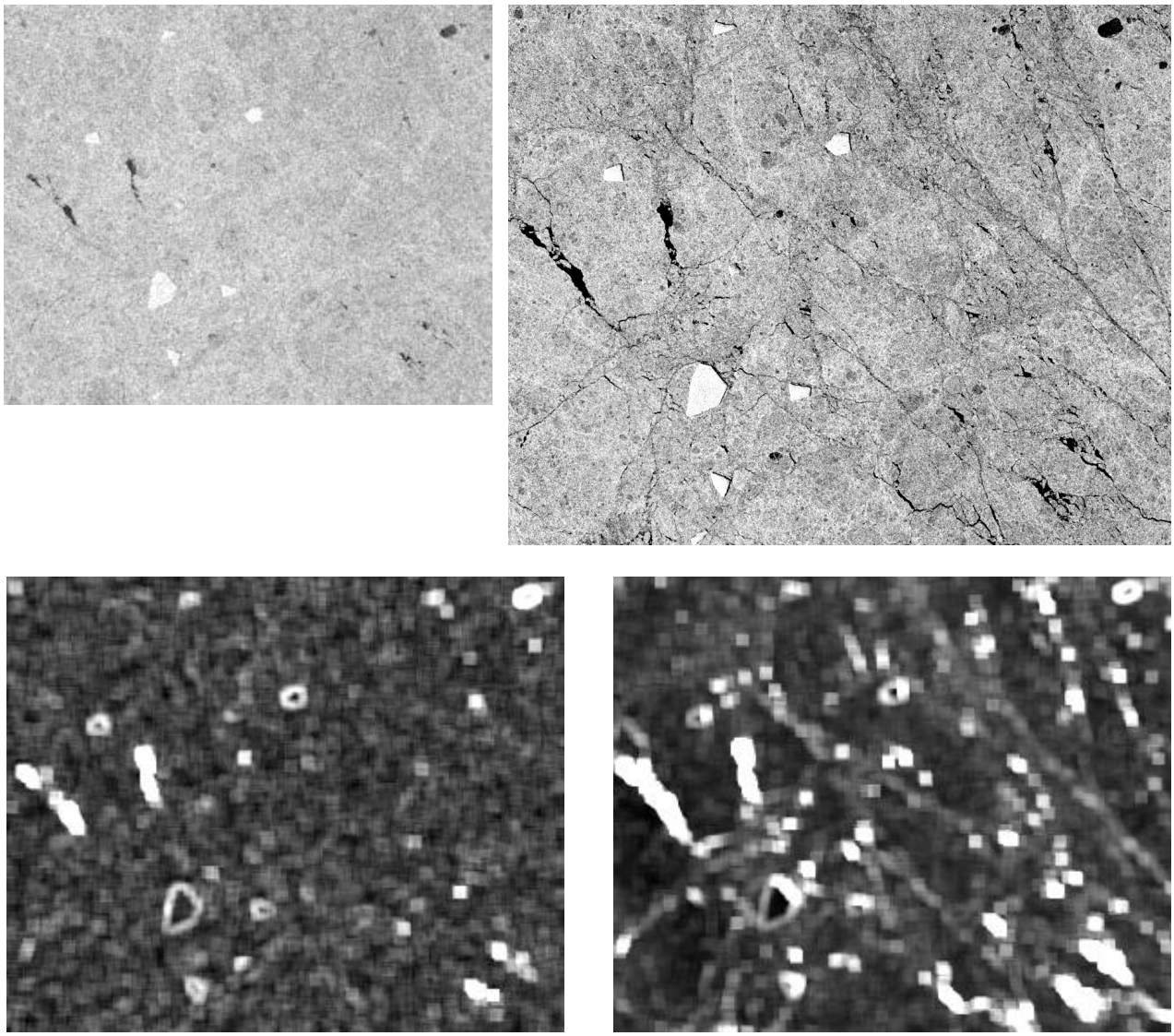

Figure 6. Texture and spatial resolution. Top left: ASAR WS image, spatial resolution 100 m, width 30 km. Top right: corresponding TSX ScanSAR, spatial resolution 30 m. Bottom left: Standard deviation for ASAR image calculated using 7×7 window. Bottom right: Standard deviation for TSX-image using 23 × 23 window. The data were acquired during the JASPER campaign over the Weddell Sea.

that spatial resolutions better than 100 m are necessary for calculating the ice displacement by correlation techniques or feature tracking. For identifying leads and polynias, the sensor should be capable of resolving areas of 0.1 km^2, i. e. length scales of 100-500 m, which requires spatial resolutions on the order of 10 m. The same is valid for the determination of iceberg sizes from SAR images. (Scales and grid dimensions cited above were taken from Table 2.2 in [11]).

In reports such as [11], the observations of single parameters (such as sea ice extent, concentration, type, drift, thickness) are treated as isolated tasks. However, by combining the observations of different parameters, a more detailed "picture" of the ice conditions is achieved which may facilitate the analysis. Different ice zones, e. g., can be better separated in coarse-resolution images if we have information about ice concentration or the presence of leads and ridges from other data sources. If, e. g. ridges are too small to be recognizable in the coarse-resolution image it is not possible to decide whether the intensity of a pixel is from a homogeneous area or includes signature contributions from ridges. As we saw above, the classification of ice types and the assessment of ice conditions in general may gain from a combination of images with different spatial resolutions.

8. CONCLUSIONS

In this paper, we discussed aspects of combining SAR imagery acquired with only small time differences at

different spatial resolutions. The higher-resolution images (pixel sizes between a few meters to a few tens of meters, and a coverage of a few tens to at maximum 200 km) serve as valuable basis for the separation of ice classes at coarser spatial resolution (> 100 m pixel size) over a larger area (> 400 km). We distinguish between a zonal classification, in which the ice cover is separated into extended segments covering several image pixels, and the identification of small or narrow structures with sizes or widths on the order of the pixel size. In the former case, it can be of advantage to use either coarse-resolution or highly averaged images (pixel sizes > 100 m) for fixing intensity thresholds between different ice classes. For the identification of narrow deformation structures such as ridges, cracks, shear zones, rafting, or smaller objects such as leads, icebergs, or belts of brash ice, spatial resolutions around 10 m are required. In case of sea ice classification, such structural elements provide a means to include texture parameters as criteria for ice type separation. In case that coarse-resolution images are employed for zonal classification, information on structural elements helps to assess their contribution to the average intensity. For practical applications, it is recommended to combine coarse-resolution C-band imagery with high-resolution X-band data, since the information content carried at both frequency bands is equivalent in many cases. This can be tested by using a conditional 2-D PDF.

For sea ice monitoring, it is essential to combine the imagery / data of different satellite sensors to improve the information retrieval on ice conditions and various ice parameters. It was, e. g., already shown that the joint use of L- and C-band SAR increases the accuracy of sea ice classification [3]. Here, we emphasized the advantages of combining images of different spatial resolutions (and areal coverage). Another scenario is the linking of radar and optical/infrared data. Sea ice conditions often change fast (within hours). This means that strategies have to be developed to coordinate data acquisitions of different satellite missions to make full use of the technological potential of the available satellite sensors.

9. ACKNOWLEDGMENT

Data were provided by the following projects: ESA Envisat/ALOS AO3545, Radarsat-2 SOAR Project 802, and TerraSAR-X OCE0078, which the author gratefully acknowledges.

10. REFERENCES

1. Marceau, D. J., & Hay, G. J. (1999), Remote sensing contributions to the scale issue. *Canadian J. Rem. Sensing*, Vol. 25, No. 4, 357-366.

2. Dierking, W. (2013). Sea ice monitoring by synthetic aperture radar. *Oceanography* 26(2)

3. Dierking, W. (2010). Mapping of different sea ice regimes using images from Sentinel-1 and ALOS synthetic aperture radar. *IEEE Trans. Geosci. Rem. Sensing*, Vol. 48, No. 3, 1045-1058

4. Hollands, T., & Dierking, W. (2011). Performance of a multi-scale correlation algorithm for the estimation of ice drift from SAR images: Initial results. *Annals of Glaciology* 52(57), 311-317

5. Weiss. J. (2013). *Drift, deformation, and fracture of sea ice – a perspective across scales*. Springer Briefs in Earth Sciences, Springer

6. Dierking, W., & Dall., J. (2008). Sea ice deformation state from synthetic aperture radar imagery – part II: effects of spatial resolution and noise level, *IEEE Trans. Geosci. Rem. Sensing*, Vol. 46, No. 8, 2197-2207

7. Narayanan, R. M., Desetty, M. K., & Reichenbach, S. E. (2002). Effect of spatial resolution on information content characterization in remote sensing imagery based on classification accuracy. *Int. J. Rem. Sensing*, Vol. 23, No. 3, 537-553.

8. Aiazzi, B., Alparone, L., & Baronti, S. (2004), Information-theoretic heterogeneity measurement for SAR imagery. *IEEE Trans. Geosci. Rem. Sensing*, Vol. 43, No. 3, 619-624

9. Le Hégarat-Mascle, S., Vidal-Madjar, D., Taconet, O., & Zribi, M. (1997). Application of Shannon information theory to a comparison between L- and C-band SIR-C polarimetric data versus incidence angle. *Rem. Sens. Environm.* 60, 121-130.

10. Barber, D. G., Shokr, M. E., Fernandes, R. A., Soulis, E. D., Flett, D. G., & LeDrew, E. F. (1993). A comparison of second-order classifiers for SAR sea ice discrimination. *Photogrammetric Engineering & Remote Sensing*, Vol. 59, No. 9, 1397-1408

11. Rott, H., Nagler, T., & Malenovský, Z. (2012). *SEN4SCI – Assessing product requirements for the scientific exploitation of the Sentinel missions: The science needs for cryosphere Sentinel 1-2-3 products.* Report Remote Sensing Laboratories, University of Zurich.